

TUM P-TH-96/79. August, 1996

# $t\bar{t}$ Production Rates at the Tevatron and the LHC in Topcolor-Assisted Multiscale Technicolor Models

Chong-Xing Yue<sup>a,b</sup>, Hong-Yi Zhou<sup>a,c</sup>, Yu-Ping Kuang<sup>a,c</sup>, Gong-Ru Lu<sup>a,b</sup><sup>a</sup>China Center of Advanced Science and Technology (World Laboratory),

P.O. Box 8730, Beijing 100080, China

<sup>b</sup>Physics Department, Henan Normal University, Xinxiang, Henan 453002, P.R. China<sup>c</sup>Institute of Modern Physics, Tsinghua University, Beijing 100084, China

## Abstract

We study the contributions of the neutral pseudo Goldstone bosons (technipions and top-pions) to the  $t\bar{t}$  production cross sections at the Tevatron and the LHC in topcolor-assisted multiscale technicolor (TOPCMTC) models via the gluon-gluon fusion process from the loop-level couplings between the pseudo Goldstone bosons and the gluons. The MRSet A<sup>0</sup> parton distributions are used in the calculation. It is shown that the new CDF datum on the  $t\bar{t}$  production cross section gives constraints on the parameters in the TOPCMTC models. With reasonable values of the parameters in TOPCMTC models, the cross section at the Tevatron is larger than that predicted by the standard model, and is consistent with the new CDF data. The enhancement of the cross section and the resonance peaks at the LHC are more significant, so that it is testable in future experiments.

PACS numbers: 12.60.Nz, 14.65.Ha, 13.87.Ce

Typeset Using REVTeX

---

 Mailing address.

## 1. Introduction

Among the yet discovered fermions, the top quark has the strongest coupling to the electroweak symmetry breaking (EW SB) sector. So that processes with top quarks are good places for probing the EW SB mechanism. Experimental measurements of the top quark mass  $m_t$  and the  $t\bar{t}$  production cross section  $\sigma_{t\bar{t}}$  at the Fermilab Tevatron have been improving. In the new 1996 CDF data [2],  $m_t = 175.6 \pm 5.7(\text{stat}) \pm 7.1(\text{syst}) \text{ GeV}$  and  $\sigma_{t\bar{t}} = 7.5^{+1.9}_{-1.6} \text{ pb}$ , the error bars are well reduced relative to the 1995 data by the CDF and D0 Collaborations [1]<sup>2</sup>. The above experimental value of  $\sigma_{t\bar{t}}$  is slightly larger than the standard model (SM) predicted value (taking into account of resummation of soft gluon contributions) which is around 5 pb [3]. Of course, one should wait for further improved data to see whether this really means something. But, as the study of the EW SB mechanism, it is interesting to study the  $t\bar{t}$  production cross section in EW SB mechanisms other than the SM Higgs sector, and see if the present experimental data can give constraints on the parameters in the EW SB models.

Technicolor (TC) [4] is an interesting idea for naturally breaking the electroweak gauge symmetry to give rise to the weak-boson masses. It is one of the important candidates for the mechanism of electroweak symmetry breaking. Introducing extended technicolor (ETC) [5] provides the possibility of generating the masses of ordinary quarks and leptons. The original ETC models suffer from the problem of predicting too large flavor changing neutral currents. It has been shown, however, that this problem can be solved in walking technicolor (WTC) theories [6]. The electroweak parameter  $S$  in WTC models is smaller than that in the simple QCD-like ETC models and its deviation from the experimental central value

---

<sup>2</sup>The 1996 D0 data still contains rather large error bars.

may fall within current experimental bounds [7]. To explain the large hierarchy of the quark masses, multiscale WTC (MWTC) model was further proposed [8]. However, even in this model, it is difficult to generate such a large top-quark mass as what is measured at the Tevatron [2] without exceeding the experimental constraint on the electroweak parameter  $T$  [9] even with "strong" ETC [10]. In addition, this model generates too large corrections to the  $Z \rightarrow b\bar{b}$  branching ratio  $R_b$  compared with the LEP data [11] due to the smallness of the decay constant  $F_0$ , and a consistent value of  $R_b$  can be obtained [12]<sup>3</sup> by combining this model with the topcolor interactions for the third generation quarks [13] at the energy scale of about 1 TeV. Similar to QCD, topcolor-assisted multiscale technicolor (TOPCMTC) theory predicts certain pseudo Goldstone bosons (PGB's) including technipions and top-pions [8] [15] [16] which can be the characteristics of this theory.

In the SM,  $t\bar{t}$  production at the Tevatron energy is dominated by the sub-process  $q\bar{q} \rightarrow t\bar{t}$  [3]. However, in a recent interesting paper, Eichten and Lane [17] showed that, in TC theories, color-octet technipions  $\pi^{0a}$  could make important contributions to  $t\bar{t}$  production at the Tevatron via the gluon-gluon fusion sub-process  $g\bar{g} \rightarrow \pi^{0a} \rightarrow t\bar{t}$  due to the large triangle-loop gluon-gluon-PGB coupling [cf. Fig. 1(a)], and such PGB could be tested by measuring the differential cross section<sup>4</sup>. Considering the total  $t\bar{t}$  production cross section, the color-singlet technipion  $\pi^0$  also contributes. Furthermore, apart from the technifermion-loop contributions considered in Ref. [17] [Fig. 1(a)], the isospin-singlet PGB's  $\pi^{0a}$  and  $\pi^0$  can also couple to the gluons through the top-quark triangle-loop [20], and make

---

<sup>3</sup>It has been shown that ETC models without exact custodial symmetry may give rise to consistent values of  $R_b$  [14], but such models may make the electroweak parameter  $T$  too large.

<sup>4</sup>The contribution of color-octet technipions to the  $t\bar{t}$  production has been considered in Refs. [8] [18] [19].

contributions shown in Fig.1 (b). In the TOPCM TC theory, the top-pion  $\pi_t^0$ , as an isospin-triplet, can couple to the gluons through the top-quark triangle-loop in an isospin-violating way similar to the coupling of  $\pi^0$  to the gluons in the Gross-Treiman-Wilczek formula [21], and the large isospin violation  $\frac{m_t - m_b}{m_t + m_b} \approx 1$  makes its contribution to the  $t\bar{t}$  production cross section important as well [cf. Fig. 1 (b)]. In this paper we study all these contributions to the production cross section of the sub-process  $gg \rightarrow t\bar{t}$ , and use the MRS set A<sup>0</sup> parton distributions [22] to calculate the cross sections at both the Tevatron and the LHC. The results of the total production cross sections show that, with these contributions, the cross section at the Tevatron is consistent with the new CDF datum for a certain range of the parameters, and the new CDF datum does give constraints on the parameters in TOPCM TC models. The cross section at the 14 TeV LHC is significantly larger than the SM prediction. The results of the differential cross sections show clear resonances of the PGB  $\pi^{0a}$  if its mass is in the reasonable range 400–500 GeV. Therefore, this kind of model can be clearly tested by future experiments.

This paper is organized as follows: Sec. 2 is devoted to the calculation of the  $gg \rightarrow t\bar{t}$  amplitude contributed by the PGB's  $\pi^{0a}$ ;  $\pi^0$ ; and  $\pi_t^0$ . In Sec. 3, we present the numerical results of the total contributions of  $\pi^{0a}$ ;  $\pi^0$  and  $\pi_t^0$  to the  $t\bar{t}$  production cross sections at the Tevatron and the LHC in TOPCM TC models considering all fermion loops in Fig. 1 (a)–(b). The conclusions are given in Sec. 4.

## 2. The $gg \rightarrow t\bar{t}$ amplitude contributed by $\pi^{0a}$ ; $\pi^0$ , and $\pi_t^0$

In the topcolor-assisted multiscale technicolor theory, there are a lot of PGB's. What are relevant to the  $t\bar{t}$  production process are the neutral technipions  $\pi^{0a}$ ;  $\pi^0$ , and the neutral top-pion  $\pi_t^0$ . In the MW TC sector, the masses of  $\pi^{0a}$  and  $\pi^0$  have been estimated to be

$M_{\phi_a} = 200 - 600 \text{ GeV}$  and  $M_{\phi_0} = 100 - 300 \text{ GeV}$ , and the decay constants are  $F = F_0 = F_L = 30 - 50 \text{ GeV}$  [8]. In the topcolor sector, if the topcolor scale is of the order of  $1 \text{ TeV}$ , the mass of  $\phi_t^0$  is around  $200 \text{ GeV}$  and its decay constant is  $F_t = 50 \text{ GeV}$  [13]. Since these PGB masses are not far from the  $t\bar{t}$  threshold and  $F, F_t$  are all small, they may give important contributions to the  $t\bar{t}$  production rates. In this section, we give the formulae for calculating the production amplitudes  $gg \rightarrow \phi_a \rightarrow t\bar{t}$ ,  $gg \rightarrow \phi_t^0 \rightarrow t\bar{t}$ , and  $gg \rightarrow \phi_t^0 \rightarrow t\bar{t}$  shown in Fig. 1 (a) and Fig. 1 (b). These concern the couplings of the PGB's to fermions and to gluons, and the PGB propagators.

In the TOPCMTC theory, the top- and bottom-quark masses  $m_t$  and  $m_b$  come from both the top-quark condensate and the ETC sector. It can be made that the large  $m_t$  is mainly contributed by the top-quark condensate, so that the ratio between the ETC contributed top- and bottom-quark masses  $m_t^0$  and  $m_b^0$  is about the same as the ratio between the charm- and strange-quark masses, i.e.  $(m_t^0/m_b^0) = (m_c/m_s) = 10$ . This makes the value of the electroweak parameter  $T$  not too large in this theory. The value of  $m_t^0$  ( $m_b^0$ ) depends on the parameters in the TOPCMTC model. For reasonable values of the parameters,  $m_t^0 = 20 - 50 \text{ GeV}$  [13].

We first consider the couplings of the PGB's to  $t\bar{t}$ . At the relevant energy scale, the PGB's can be described by local fields. In the MWTC theory, the coupling of technipions to fermions are induced by ETC interactions and hence are model dependent. However, it has been generally argued that the couplings of the PGB's to the quark  $q$  and antiquark  $\bar{q}$  are proportional to  $m_q^0/F$  [17] [23] [18], where  $m_q^0$  is the part of the quark mass acquired from the ETC. The PGB- $q\bar{q}$  vertices are of the following forms [17] [18]:

$$\frac{C_q m_q^0}{F} \phi_a^0 (q \gamma^5 \bar{q}); \quad \frac{C_q m_q^0}{F} \phi_a^0 (q \gamma^5 \frac{\lambda^a}{2} \bar{q}); \quad (1)$$

where  $\lambda^a$  is the Gell-Mann matrix of the color group,  $C_q$  is a model dependent coupling

constant which is expected to be typically of  $O(1)$  [17] [23] [18]. In the topcolor sector, by similar argument, we can obtain the interactions of the top-pions with the top and bottom quarks by replacing  $m_q^0$  by  $m_q - m_q^0$ , and  $F$  by  $F_t$  in (1), i.e. [16]

$$\frac{m_t - m_t^0}{2F_t} t_5 t^0 + \frac{i}{2} [t(1 - \gamma_5)b + \frac{1}{2} b(1 + \gamma_5)t]; \quad (2)$$

$$\frac{m_b - m_b^0}{2F_t} b_5 b^0; \quad (3)$$

Next we consider the couplings of the  $PG B$ 's to the gluons. Consider a general formula for the coupling of a  $PG B$  to two gauge fields  $B_1$  and  $B_2$ . As far as the  $PG B$ 's are described by local fields, the triangle fermion loops coupling the  $PG B$ 's to  $B_1$  and  $B_2$  can be evaluated from the Adler-Bell-Jackiw anomaly. The general form of the effective  $PG B-B_1-B_2$  interaction is [24] [18]

$$\frac{1}{(1 + \gamma_{B_1 B_2})} \frac{S_{B_1 B_2}}{4 F^2} (\partial_{B_1}) (\partial_{B_2}); \quad (4)$$

where  $\gamma$  stands for  $^0$ ,  $^{0a}$  or  $^0_t$ ; and when  $B_1$  and  $B_2$  are gluons, the factors  $S_{gg}$  in different cases are as follows.

For  $^0$  and  $^{0a}$  with technifermion triangle-loop [24],

$$S_{^0_{g_b g_c}}^{(Q, L)} = \frac{P}{2} g_s^2 N_{TC} \gamma_{bc}; \quad S_{^{0a}_{g_b g_c}}^{(Q, L)} = \frac{P}{2} g_s^2 N_{TC} d_{abc}; \quad (5)$$

For  $^0$  and  $^{0a}$  with top-quark triangle-loop [20],

$$S_{^0_{g_b g_c}}^{(t)} = \frac{C_t}{2} g_s^2 J(R_{^0})_{bc}; \quad S_{^{0a}_{g_b g_c}}^{(t)} = \frac{C_t}{2} g_s^2 d_{abc} J(R_{^{0a}}); \quad (6)$$

with

$$J(R_{^0}) = \frac{m_t^0}{m_t} \frac{1}{R^2} \int_0^1 \frac{dx}{x(1-x)} \ln[1 - R^2 x(1-x)]; \quad (7)$$

where  $R = \frac{M}{m_t}$ .

The coupling of  $\phi_t^0$  to gluons via the top-quark triangle-loop is isospin-violating similar to the coupling of  $\phi^0$  to gluons in the Gross-Treiman-Wilczek formula [21]. It can also be calculated from the formula in Ref. [20] which gives<sup>5</sup>

$$S_{\phi_t^0 g_b g_c} = \frac{1}{2} g_s^2 J(R_{\phi_t^0}); \quad (8)$$

with

$$J(R_{\phi_t^0}) = \frac{m_t}{m_t} \frac{m_t^0}{R_{\phi_t^0}^2} \frac{1}{0} \int_0^1 \frac{dx}{x(1-x)} \ln[1 - R_{\phi_t^0}^2 x(1-x)]; \quad (9)$$

where  $R_{\phi_t^0} = \frac{M_{\phi_t^0}}{m_t}$ .

Finally the  $(\phi^0; \phi_a^0; \text{or } \phi_t^0)$  propagator in Fig. 1 takes the form

$$\frac{i}{\hat{s} - M^2 + iM}; \quad (10)$$

where  $\sqrt{\hat{s}}$  is the cm. energy and  $M$  is the total width of the PGB. The  $iM$  term in (11) is important when  $\hat{s}$  is close to  $M^2$ . The widths  $\Gamma_{\phi^0}; \Gamma_{\phi_a^0}$ , and  $\Gamma_{\phi_t^0}$  can be obtained as follows.

From (1) and (4) we see that the dominant decay modes of  $\phi^0$  are  $\phi^0 \rightarrow b\bar{b}$  and  $\phi^0 \rightarrow gg$ . So that

$$\Gamma_{\phi^0} = \Gamma(\phi^0 \rightarrow b\bar{b}) + \Gamma(\phi^0 \rightarrow g_a g_b); \quad (11)$$

From (1) and (5), we can obtain

$$\Gamma(\phi^0 \rightarrow b\bar{b}) = \frac{3C_b m_b^0 M}{16 F^2} \sqrt{1 - \frac{4m_b^2}{M^2}}; \quad (12)$$

and

---

<sup>5</sup> It is proportional to the isospin-violating factor  $\frac{m_t - m_b}{m_t + m_b} \approx 1$ .

$$\begin{aligned}
(\pi^0 \rightarrow g_a g_b) &= (Q_{\pi^0}) (\pi^0 \rightarrow g_a g_b) + (t) (\pi^0 \rightarrow g_a g_b) = (Q_{\pi^0}) (\pi^0 \rightarrow g_a g_b) \left[ 1 + \frac{C_t J(R_{\pi^0})^2}{2N_{TC}} \right] \\
&= \frac{s N_{TC}^2}{16^3} \frac{M^3}{F^2} \left[ 1 + \frac{C_t J(R_{\pi^0})^2}{2N_{TC}} \right]; \tag{13}
\end{aligned}$$

where  $(Q_{\pi^0})$  and  $(t)$  are the  $\pi^0 \rightarrow gg$  rates contributed by the technifermion loop and top-quark loop, respectively.

It has been shown [20] [25] that  $\pi_{0a}$  decays dominantly into  $tt$ ,  $gg$ , and  $gZ$ . So that

$$\Gamma_{\pi_{0a}} = (\pi_{0a} \rightarrow bb) + (\pi_{0a} \rightarrow g_a g_b) + (\pi_{0a} \rightarrow tt) + (\pi_{0a} \rightarrow gZ); \tag{14}$$

From (1), (4) and the value of  $S(\pi_{0a} gZ)$  given in Ref. [23] [18], we can obtain

$$(\pi_{0a} \rightarrow qq) = \frac{C_q}{16} \frac{m_q^2 M_{\pi_{0a}}}{F^2} \frac{V_{uq}^2}{t} \left[ 1 - \frac{4m_q^2}{M_{\pi_{0a}}^2} \right]; \quad q = t, b; \tag{15}$$

$$\begin{aligned}
(\pi_{0a} \rightarrow g_a g_b) &= (Q_{\pi^0}) (\pi_{0a} \rightarrow g_a g_b) \left[ 1 + \frac{C_t J(R_{\pi_{0a}})^2}{2^2 2N_{TC}} \right] \\
&= \frac{5}{384} \frac{s N_{TC}^2}{3} \frac{M_{\pi_{0a}}^3}{F^2} \left[ 1 + \frac{C_t J(R_{\pi_{0a}})^2}{2^2 2N_{TC}} \right]; \tag{16}
\end{aligned}$$

$$(\pi_{0a} \rightarrow gZ) = \frac{s}{144^3} \frac{N_{TC}}{4} \tan^2 \theta_w \frac{M_{\pi_{0a}}^3}{F^2}; \tag{17}$$

Since the top-pion mass is around 200 GeV, it decays mainly into  $bb$  and  $gg$ . Thus

$$\Gamma_{\pi_t^0} = (\pi_t^0 \rightarrow b\bar{b}) + g (\pi_t^0 \rightarrow g_a g_b); \tag{18}$$

From (1) and (4) we obtain

$$(\pi_t^0 \rightarrow b\bar{b}) = \frac{3}{16} \frac{(m_b - m_b^0)^2}{F_t^2} M_{\pi_t^0} \frac{V_{ub}^2}{t} \left[ 1 - \frac{4m_b^2}{M_{\pi_t^0}^2} \right]; \tag{19}$$

and

$$g_t^0 \rightarrow g_a g_b = \frac{2}{64} \frac{M_{0t}^3}{F_t^2} J(R_{0t})^2 : \quad (20)$$

With the above formulae, we can obtain the following production amplitudes.

$$\begin{aligned} A(g_b g_c \rightarrow 0_a \rightarrow tt) &= A^{(Q, L)}(g_b g_c \rightarrow 0_a \rightarrow tt) + A^{(t)}(g_b g_c \rightarrow 0_a \rightarrow tt) \\ &= \frac{C_t m_t^0 g_s^2 N_{TC} + C_t J(R_{0a}) = 2}{4 \cdot 2 \cdot 2 F_t^2 [\mathcal{S} M_{0a} + i M_{0a}]} (t \rightarrow \frac{a}{2} t) k_1 k_2 \rightarrow 12 ; \end{aligned} \quad (21)$$

$$\begin{aligned} A(g_b g_c \rightarrow 0 \rightarrow tt) &= A^{(Q, L)}(g_b g_c \rightarrow 0 \rightarrow tt) + A^{(t)}(g_b g_c \rightarrow 0 \rightarrow tt) \\ &= \frac{1}{2} \frac{C_t m_t^0 g_s^2 N_{TC} + C_t J(R_{0a}) = 2}{4 \cdot 2 \cdot 2 F_t^2 [\mathcal{S} M_{0a} + i M_{0a}]} (t \rightarrow t) k_1 k_2 \rightarrow 12 ; \end{aligned} \quad (22)$$

and

$$A(g_b g_c \rightarrow 0_t \rightarrow tt) = \frac{1}{2} \frac{(m_t - m_t^0) g_s^2 J(R_{0t})}{8 \cdot 2 F_t^2 [\mathcal{S} M_{0t}^2 + i M_{0t}]} (t \rightarrow t) k_1 k_2 \rightarrow 12 : \quad (23)$$

It is easy to obtain the SM tree-level  $tt$  production amplitudes

$$A_{\text{tree}}^{\text{SM}}(qq \rightarrow tt) = \frac{ig_s^2 v(p_q) \frac{a}{2} u(p_q) u(p_t) \frac{a}{2} v(p_t)}{\mathcal{S}} ; \quad (24)$$

and

$$A_{\text{tree}}^{\text{SM}}(gg \rightarrow tt) = A_{\text{tree}}^{\text{SM}(s)}(gg \rightarrow tt) + A_{\text{tree}}^{\text{SM}(t)}(gg \rightarrow tt) + A_{\text{tree}}^{\text{SM}(u)}(gg \rightarrow tt) ; \quad (25)$$

with

$$A_{\text{tree}}^{\text{SM}(s)}(gg \rightarrow tt) = ig_s^2 [(k_2 - k_1) \cdot (p_2 - p_1) + (k_2 + 2k_1) \cdot p_2 - (2k_2 + k_1) \cdot p_1] ;$$

$$\frac{1}{\mathcal{S}} u(p_t) \cdot (if_{abc} \frac{c}{2}) v(p_t) ; \quad (26)$$

$$A_{\text{tree}}^{\text{SM}(t)}(gg \rightarrow tt) = ig_s^2 \frac{u(p_t)/1 \cdot (q - m_t)/2 \cdot \frac{b}{2} \cdot \frac{a}{2} v(p_t)}{q^2 - m_t^2} ; \quad q = p_t - k_1 ; \quad (27)$$

$$A_{\text{tree}}^{\text{SM}(u)}(gg \rightarrow t\bar{t}) = A_{\text{tree}}^{\text{SM}(t)}(gg \rightarrow t\bar{t}) [1 \pm 2(a \pm b)]; \quad (28)$$

where  $k_1, k_2$  are the momenta of the two initial-state gluons,  $p_t$  is the momentum of the top-quark.

Adding all these amplitudes together, we obtain the total  $t\bar{t}$  production amplitude.

### 3. The $t\bar{t}$ production cross sections at the Tevatron and the LHC

Once we have the cross section at the parton level  $\hat{\sigma}$ , the cross section at the hadron collider is obtained by convoluting it with the parton distributions [26]

$$\sigma(pp \rightarrow t\bar{t}) = \sum_{ij} \int_0^1 dx_i dx_j f_i^{(p)}(x_i; Q) f_j^{(\bar{p})}(x_j; Q) \hat{\sigma}(ij \rightarrow t\bar{t}); \quad (29)$$

where  $i, j$  stand for the partons  $g, q$  and  $\bar{q}$ ;  $x_i$  is the fraction of the longitudinal momentum of the proton (antiproton) carried by the  $i$ -th parton;  $Q^2 = s$ ; and  $f_i^{(p)}$  is the parton distribution functions in the proton (antiproton). In this paper, we take the MRS set A<sup>0</sup> parton distribution for  $f_i^{(p)}$ . Taking into account of the QCD corrections, we shall multiply the obtained  $\sigma$  by a factor 1.5 [3] as what was done in Ref. [17].

The main purpose of Ref. [17] is to show the signal of  $\phi_a^0$  at the Tevatron, so that they only calculated the technifermion-loop contributions and neglected the interference between  $A_{\text{tree}}^{\text{SM}}(gg \rightarrow t\bar{t})$  and  $A(g_b g_c \rightarrow \phi_a^0 \rightarrow t\bar{t})$  as a first investigation. In this section, we present the cross sections at the Tevatron and the LHC in TOPCMTC models considering the contributions of  $\phi_a^0$ ,  $\phi^0$  and  $\phi_t^0$  from Fig. 1(a) and Fig. 1(b) with the interferences taken into account. In our calculation, we take the more updated parton distribution functions MRS set A<sup>0</sup> instead of EHLQ set 1 taken in Ref. [17]. The fundamental SM parameters in our calculation are taken to be  $m_t = 176 \text{ GeV}$ ;  $\sin^2 \theta_W = 0.231$ , and  $\alpha_s(\sqrt{s})$  the same as that in the MRS set A<sup>0</sup> parton distributions. For the parameters in the TOPCMTC models,

we simply take  $C_t = C_b = 1$  and take the reasonable values  $F = 40 \text{ GeV}$ ,  $F_t = 50 \text{ GeV}$  in this calculation. For the technipion masses, we fix  $M_{\rho} = 150 \text{ GeV}$ , and vary  $M_{\rho a}$  from  $400 \text{ GeV}$  to  $500 \text{ GeV}$ . The values of  $m_t^0$  and  $m_t^0$  depend on the parameters in the TOPCMTC models. To see how these values affect the cross sections, we take, some reasonable values for each of them, namely  $M_{\rho} = 150 \text{ GeV}$  and  $350 \text{ GeV}$ ,  $m_t^0 = 20; 35$  and  $50 \text{ GeV}$ .

The results of the cross sections at the  $1.8 \text{ TeV}$  Tevatron are listed in Table 1, in which  $\sigma_{tt}^{(i)}$  is the TOPCMTC correction [including the interferences between the TOPCMTC amplitudes (21)–(23) and the tree-level SM amplitudes (24)–(28)] to the tree-level SM cross section in the total cross section  $\sigma_{tt}^{(i)}$ , with  $i = 1; 2; 3$  corresponding to  $m_t^0 = 20 \text{ GeV}; 35 \text{ GeV};$  and  $50 \text{ GeV}$ . We see that for most values of the parameters the cross sections  $\sigma_{tt}$  are consistent with the new CDF data except that the cross sections are too large for  $m_{\rho a} = 400 \text{ GeV}$  with  $m_t^0 = 35 \text{ GeV}$ . Therefore the CDF data does give constraints on the values of  $m_{\rho a}$  and  $m_t^0$  which depends on the specific model. To see the constraints more precisely, we plot the cross section versus  $m_t^0$  in Fig. 2 (with  $m_{\rho} = 150 \text{ GeV}$ ) and Fig. 3 (with  $m_{\rho} = 350 \text{ GeV}$ ), in which the solid, dashed and, dotted lines stand for  $m_{\rho a} = 400; 450;$  and  $500 \text{ GeV}$ , respectively. Comparing with the new CDF data (the shaded band), we see that there are parameter ranges outside the band of the CDF data, especially for  $m_t^0 = 150 \text{ GeV}$ , the range of parameters  $m_{\rho a} = 400 \text{ GeV}$  with  $m_t^0 > 30 \text{ GeV}$  is disfavored; for  $m_t^0 = 350 \text{ GeV}$ , the range of parameters  $m_{\rho a} = 400 \text{ GeV}$  with all  $m_t^0 > 20 \text{ GeV}$  is disfavored.

In Figs. 4-6, we plot the differential cross sections  $\frac{d\sigma_{tt}}{dm_{tt}}$  versus the  $tt$  invariant mass  $m_{tt}$  at the  $\sqrt{s} = 1.8 \text{ TeV}$  Tevatron for various values of the parameters. We see that clear peak of the  $\rho a$  resonance emerges when  $m_{\rho a}$  lies in the range of  $400$  to  $500 \text{ GeV}$ . The larger the value of  $m_t^0$ , the clearer the signal. This is because that the coupling in (1) is

proportional to  $m_t^0$ . For the case of  $m_{\tilde{t}}^0 = 350 \text{ GeV}$ , the  $\tilde{t}^0$  peak can also be seen. Thus the model can be tested by the differential cross section for certain values of the parameters.

In Table 2, we list the values of  $\sigma_{t\bar{t}}$  and  $\sigma_{t\bar{t}}^{\text{differential}}$  at the  $\sqrt{s} = 14 \text{ TeV}$  LHC. We see that the cross sections are much larger than those at the Tevatron due to the fact that at the LHC  $t\bar{t}$  production is dominated by gluon-fusion. The obtained cross section is significantly larger than the SM predicted value, so that it can be easily tested by the future experiment. In Figs. 7-9, we plot the differential cross sections at the LHC for various values of the parameters. We see that differential cross sections are similar to those at the Tevatron but the peaks are more significant due to the same reason. So that the models can be better tested at the LHC.

#### 4. Conclusions

In this paper, we studied the  $t\bar{t}$  production cross sections at the  $\sqrt{s} = 1.8 \text{ TeV}$  Tevatron and the  $\sqrt{s} = 14 \text{ TeV}$  LHC in the TOPCMTC models. The TOPCMTC contributions are mainly via the s-channel PGB's  $\tilde{t}^{0a}$ ;  $\tilde{t}^0$ ; and  $\tilde{t}^0$  through gluon-fusion. We calculated both the diagrams in Fig.1 (a) and Fig.1 (b), and took into account the interferences between the tree level SM amplitudes [(24)-(28)] and the TOPCMTC amplitudes [(21)-(23)]. The MRS set A<sup>0</sup> parton distribution functions are taken in this calculation. In the study, we take  $m_{\tilde{t}}^0 = 150 \text{ GeV}$  and vary other parameters in the models. Our results show that the production cross sections are enhanced by the TOPCMTC contributions. The present CDF datum on the production cross section gives constraints on the model-dependent parameters  $m_{\tilde{t}^{0a}}$  and  $m_{\tilde{t}^0}^0$ , i.e.  $m_{\tilde{t}^{0a}} = 400 \text{ GeV}$  with large  $m_{\tilde{t}^0}^0$  is disfavored. In the differential cross

sections, clear peaks of the  $\sigma_a$  and  $\sigma_t^0$  can be seen for reasonable range of the parameters, so that the models are experimentally testable at the Tevatron and the LHC. The cross section at the LHC is significantly larger than the SM predicted value, and the peaks are more significant at the LHC than at the Tevatron due to the fact that  $t\bar{t}$  production at the LHC is dominated by gluon-fusion. Therefore the models can be better tested at the LHC.

#### ACKNOWLEDGMENT

C.-X. Yue would like to thank B.-L. Young for his valuable discussions. This work is supported by National Natural Science Foundation of China, the Natural Foundation of Henan Scientific Committee, and the Fundamental Research Foundation of Tsinghua University.

#### Reference

1. F. Abe, et al. The CDF Collaboration, *Phys. Rev. Lett.* 74 (1995) 2626; S. Abachi, et al. The Collaboration *Phys. Rev. Lett.* 74 (1995) 2632.
2. G. F. Tartarelli, *Fermilab Preprint CDF/PUB/TOP/PUBLIC/3664* (1996).
3. E. Laenen, J. Smith, and W. L. van Neerven, *Phys. Lett. B* 321 (1994) 254; E. L. Berger and H. Contopanagos, *Proc. International Symposium on Heavy Flavor and Electroweak Theory, August 19-21, 1995, Beijing, China*, edited by C. H. Chang and C. S. Huang (World Scientific Pub., Singapore) pp 25-36.
4. S. Weinberg, *Phys. Rev. D* 13, 974 (1976); *ibid.* D 19, 1277 (1979);  
L. Susskind, *Phys. Rev. D* 20, 2619 (1979).
5. S. Dimopoulos and L. Susskind, *Nucl. Phys. B* 155, 237 (1979); E. Eichten and K. Lane, *Phys. Lett. B* 90, 125 (1980).

6. B. Holdom, Phys. Rev. D 24,1441 (1981); Phys. Lett.B 150,301 (1985);  
T. Appelquist, D. Karabali and L.C.R. Wijewardhana, Phys.  
Rev. Lett.57,957 (1986).
7. T. Appelquist and G. Triantaphyllou, Phys. Lett. B 278,345 (1992);  
R. Sundrum and S. Hsu, Nucl. Phys. B 391,127 (1993); T. Appelquist  
and J. Terning, Phys. B 315,139 (1993).
8. K. Lane and E. Eichten, Phys. Lett. B 222,274 (1989); K. Lane and  
M. V. Ramana, Phys. Rev. D 44,2678 (1991).
9. R. S. Chivukula, B. A. Dobrescu, and J. Terning, BUHEP-95-22, hep/9506450.
10. T. Appelquist et al, Phys. Lett. B 220,223 (1989); R. S. Chivukula,  
A. G. Gohen and K. Lane, Nucl. Phys. B 343,554 (1990).
11. The LEP Collaborations ALEPH, DELPHI, L3, OPAL and the LEP Electroweak  
Working Group, CERN Preprint CERN-PPE/95-172.
12. Chong-Xing Yue, Yu-Ping Kuang, and Gong-Ru Lu, TUM P-TM -95/72.
13. C. T. Hill, Phys. Lett. B 266,419 (1991); S. P. Martin, Phys. Rev. D 45,  
4283 (1992); D 46,2197 (1992); Nucl Phys. B 398,359 (1993); M. Linder and  
D. Ross, NuclB 370,30 (1992); C. T. Hill, D. Kennedy, T. Onogi and H. L. Yu,  
Phys. Rev. D 47,2940 (1993); W. A. Bardeen, C. T. Hill and M. Lindner,  
Phys. Rev. D 41,1649 (1990).
14. Guo-Hong Wu, Phys Rev Lett.74 (1995)4137; Chong-Xing Yue, Yu-Ping Kuang,  
Gong-Ru Lu, and Ling-De Wan, Phys. Rev. D 51,5314 (1995).

15. K . Lane, BUHEP-95-23, hep-ph/9507289.
16. C . T . Hill, Phys. Lett. B 345,483 (1995); K . Lane and E Eichten,  
Phys. Lett. B 352,382 (1995).
17. E Eichten and K . Lane, Phys. Lett. B 327,129 (1994).
18. V Lubicz, Nucl. PhysB 404,559 (1993); V . Lubiz and P . Santorelli, BUHEP-95-16,  
Napoliprep. D SF 21/95
19. B . Holdom and M . V . Ram an , Phys. Lett. B 353,295 (1995).
20. D . Slaven, Bing-Ling Young, and Xin-M in Zhang, Phys. Rev. D 45,4349 (1992);  
Chong-X ing Yue, X ue-LeiW ang and G ong-Ru Lu, J. Phys. G 19, 821 (1993).
21. D . J. G ross, S B . Treim an, and F . W ilczek, Phys. PevD 19,2188 (1979).
22. A . D . M artin, W . J. Stirling and R . G . Roberts, Phys. Lett. B 354,155 (1995).
23. L Randall and E . H . Sim nons, Nucl. PhysB 380,3 (1992).
24. S . D im opoulos, S . Raby, and G . L . Kane, Nucl. PhysB 182,77 (1981); J . Ellis, et al.,  
Nucl. PhysB 182,529 (1981).
25. Chong-X ing Yue, G ong-Ru Lu and Jin-M in Yang, M odern. Phys. LettA ,  
Vol8, 2843 (1993).
26. E . Eichten, I. H inchli e, K . Lane, and C . Quigg, Rev. M od. Phys. 56,579 (1984).

# TABLES

Table 1.  $t\bar{t}$  production cross section  $(gg \rightarrow t^{(a)}(\bar{t}^{(a)}; \bar{t}^{(a)}) \rightarrow t\bar{t})$  at the  $\sqrt{s} = 1800 \text{ GeV}$  Tevatron in the topcolor-assisted multiscale walking technicolor model with  $m_{\phi} = 150 \text{ GeV}$ .

$^{(i)}$  is the TOPCM TC correction to the tree-level SM cross section and  $_{t\bar{t}}^{(i)}$  is the total cross section, where  $i = 1; 2; 3$  correspond to  $m_t^0 = 20 \text{ GeV}; 35 \text{ GeV};$  and  $50 \text{ GeV}$ , respectively. A factor 1.5 of QCD corrections has been taken into account.

$M_t (\text{GeV})$	$M_{\phi a} (\text{GeV})$	$^{(1)}$ (pb)	$_{t\bar{t}}^{(1)}$ (pb)	$^{(2)}$ (pb)	$_{t\bar{t}}^{(2)}$ (pb)	$^{(3)}$ (pb)	$_{t\bar{t}}^{(3)}$ (pb)
150	400	2.750	7.861	5.678	10.789	7.829	12.940
150	450	1.350	6.461	2.688	7.798	3.618	8.729
150	500	0.632	5.743	1.245	6.356	1.680	6.791
350	400	4.638	9.749	7.127	12.238	8.834	13.945
350	450	2.970	8.081	3.965	9.076	4.571	9.682
350	500	2.279	7.390	2.480	7.591	2.598	7.709

Table 2.  $t\bar{t}$  production cross section  $(gg \rightarrow t^{(a)}(\bar{t}^{(a)}; \bar{t}^{(a)}) \rightarrow t\bar{t})$  at the  $\sqrt{s} = 14 \text{ TeV}$  LHC in the topcolor-assisted multiscale walking technicolor model with  $m_{\phi} = 150 \text{ GeV}$ .

$^{(i)}$  is the TOPCM TC correction to the tree-level SM cross section and  $_{t\bar{t}}^{(i)}$  is the total cross section, where  $i = 1; 2$  correspond to  $m_t^0 = 20 \text{ GeV}$  and  $35 \text{ GeV}$ , respectively. A factor 1.5 of QCD corrections has been taken into account.

$M_t (\text{GeV})$	$M_{\phi a} (\text{GeV})$	$^{(1)}$ (nb)	$_{t\bar{t}}^{(1)}$ (nb)	$^{(2)}$ (nb)	$_{t\bar{t}}^{(2)}$ (nb)
150	400	2.753	3.493	5.577	6.317
150	450	2.073	2.813	4.167	4.907
150	500	1.596	2.336	3.180	3.920
350	400	3.791	4.531	6.293	7.033
350	450	3.182	3.922	5.006	5.746
350	500	2.568	3.308	3.978	4.718

## Figure Captions

Fig. 1. Feynman diagrams for the TOPCMTC contributions to the  $t\bar{t}$  productions at the Tevatron and the LHC.

(a). Techniquark loop contributions. (b). Top-quark loop contributions.

Fig. 2. The plot of  $\sigma_{t\bar{t}}$  versus  $m_t^0$  for  $m_{\tilde{t}^0} = 150$  GeV at the Tevatron. The solid, dashed, and dotted lines stand for  $m_{\tilde{a}^0} = 400; 450; \text{ and } 500$  GeV, respectively. The CDF data is indicated by the shaded band.

Fig. 3. Same as Fig. 2 but for  $m_{\tilde{t}^0} = 350$  GeV.

Fig. 4. Differential cross section  $\frac{d\sigma_{t\bar{t}}}{dm_{t\bar{t}}}$  (in logarithmic scale) versus the  $t\bar{t}$  invariant mass  $m_{t\bar{t}}$  at the Tevatron for  $m_{\tilde{a}^0} = 400; 450; \text{ and } 500$  GeV with  $m_{\tilde{t}^0} = 150$  GeV,  $m_t^0 = 20$  GeV, and  $m_{\tilde{t}^0} = 150$  GeV.

Fig. 5. Same as Fig. 3. but with  $m_{\tilde{t}^0} = 35$  GeV and  $m_{\tilde{a}^0} = 150$  GeV.

Fig. 6. Same as Fig. 3. but with  $m_{\tilde{t}^0} = 20$  GeV and  $m_{\tilde{a}^0} = 350$  GeV.

Fig. 7. Same as Fig. 3. but at the LHC.

Fig. 8. Same as Fig. 4 but at the LHC.

Fig. 9. Same as Fig. 5 but at the LHC.

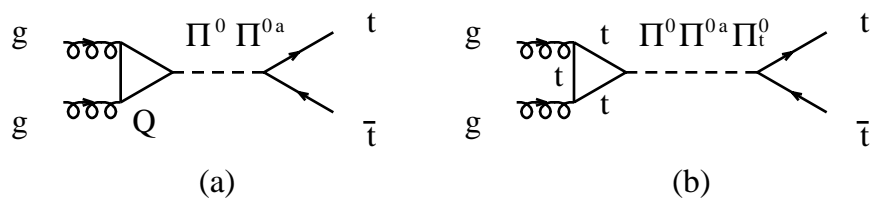


Fig. 1

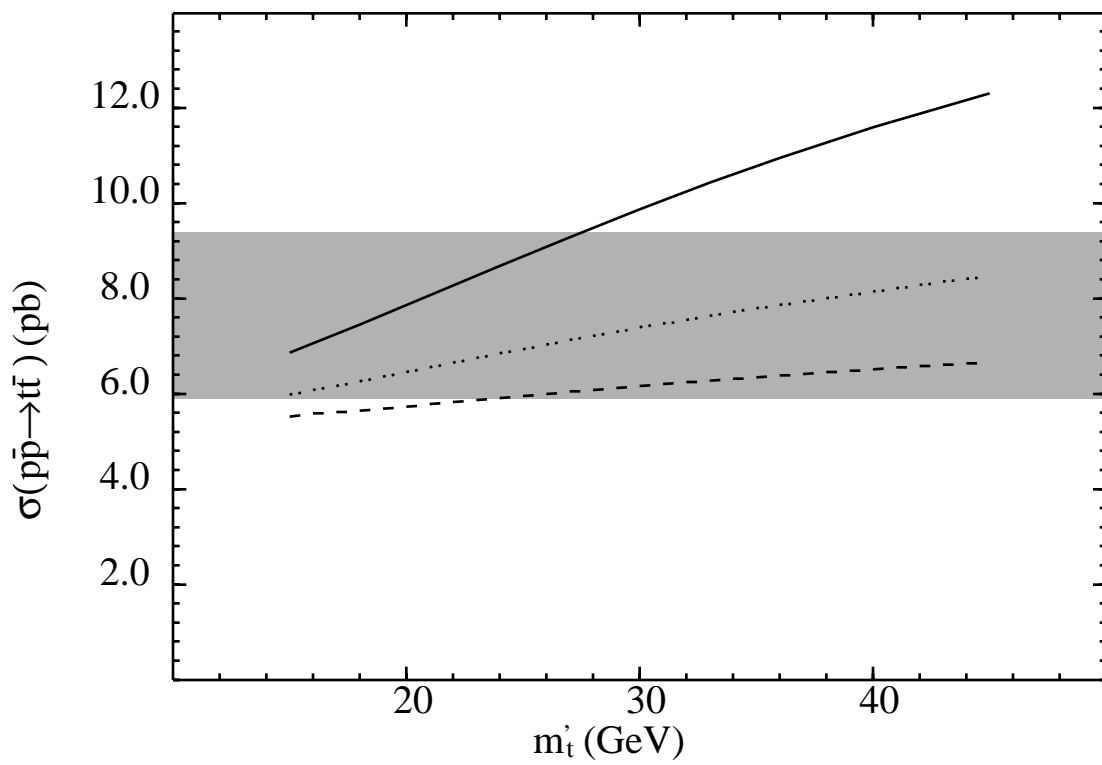


Fig. 2

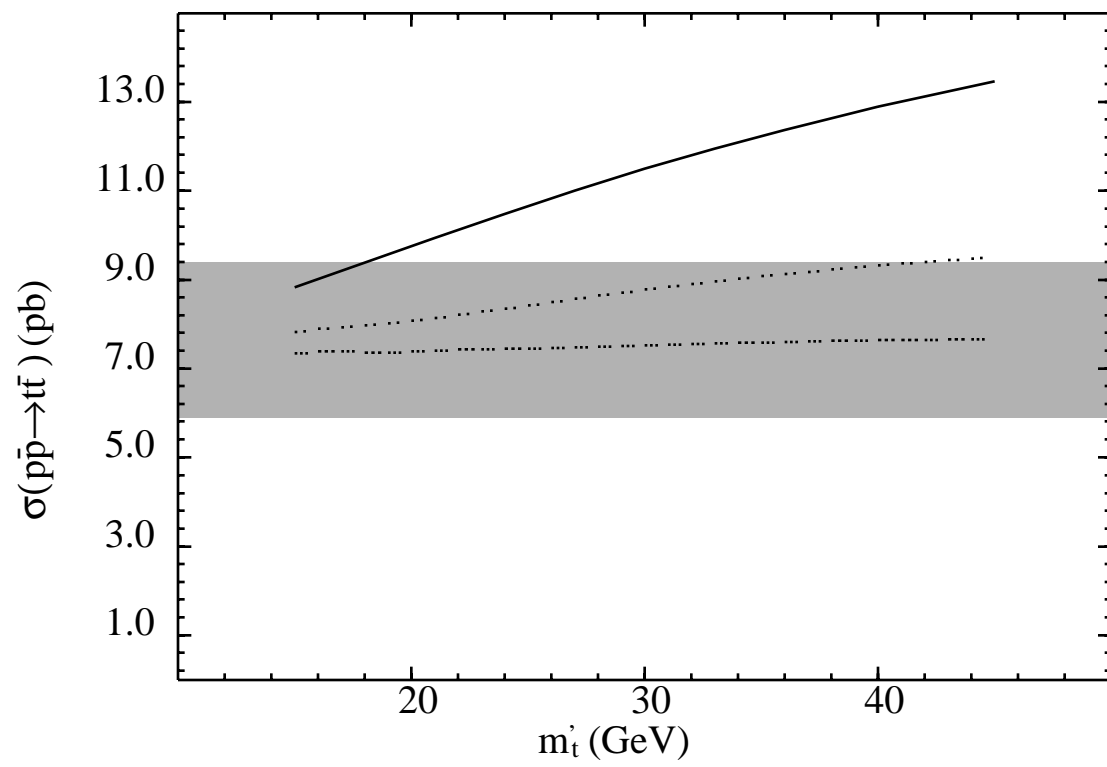


Fig.3

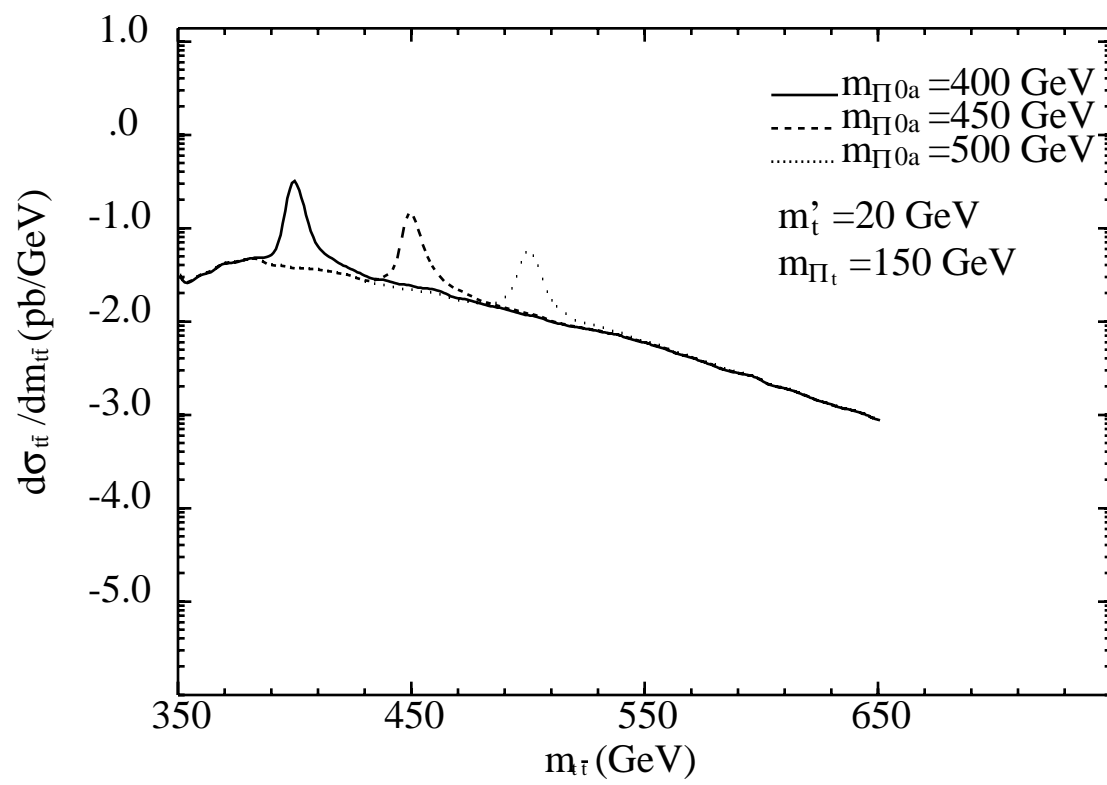


Fig. 4

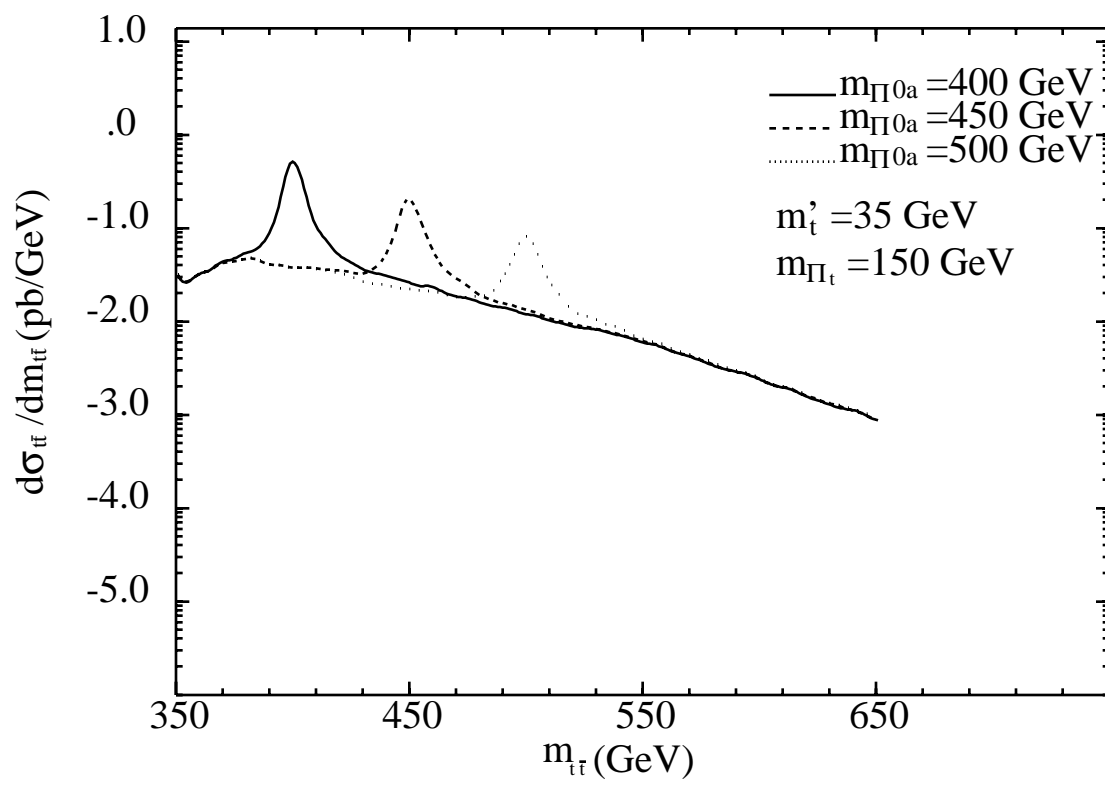


Fig. 5

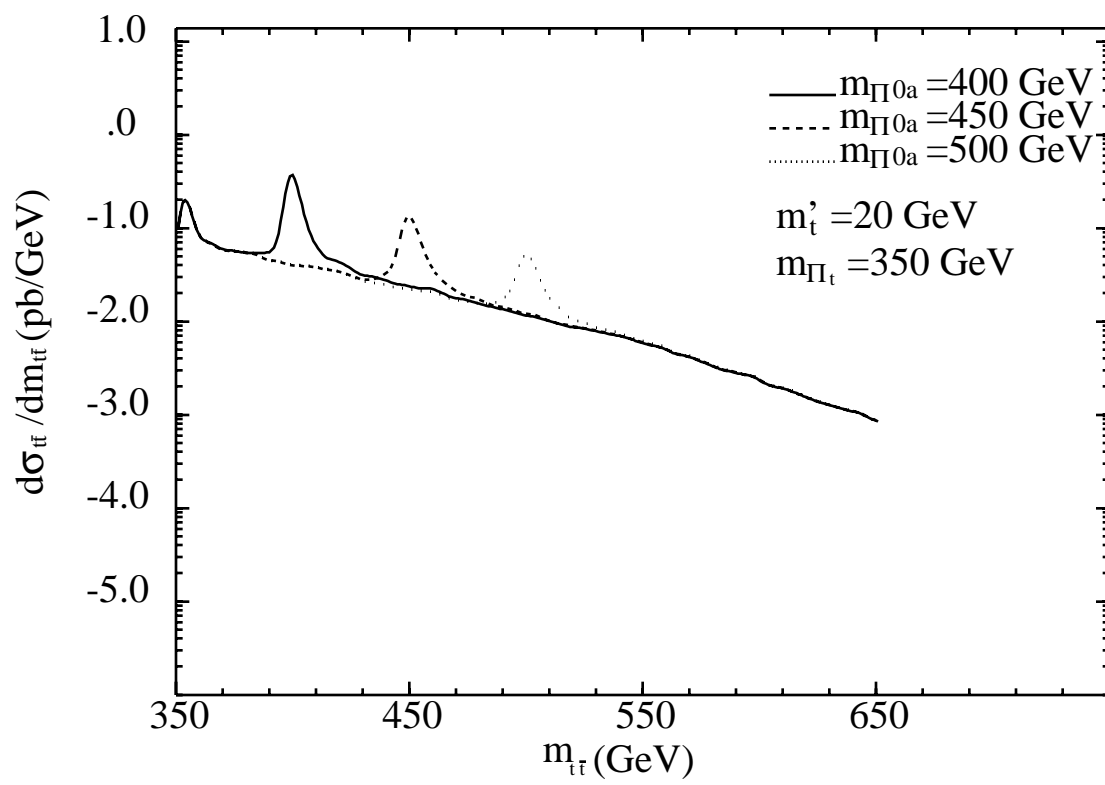


Fig. 6

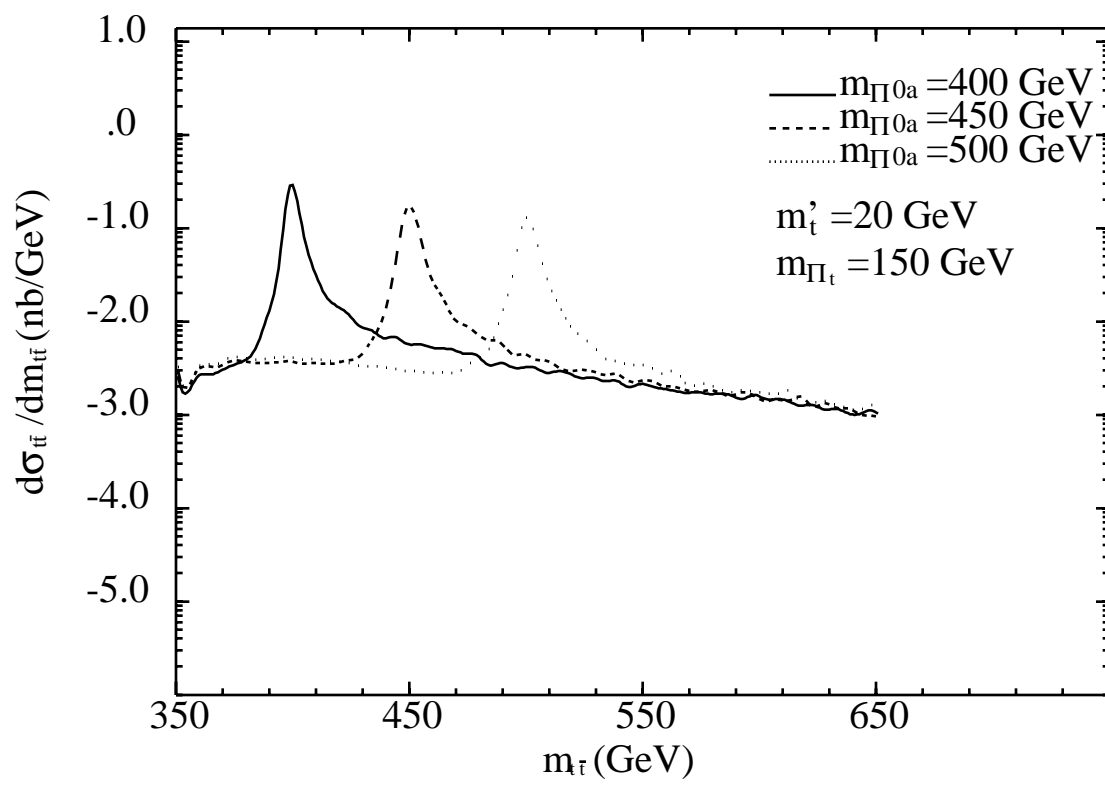


Fig. 7

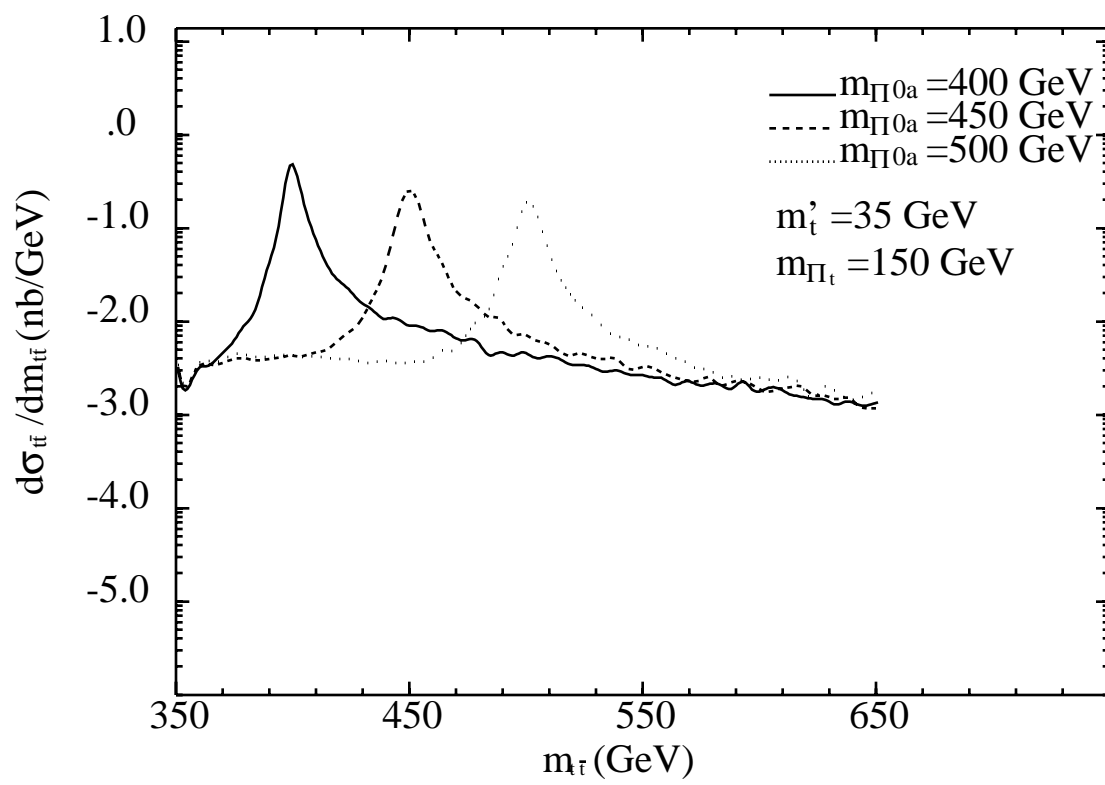


Fig. 8

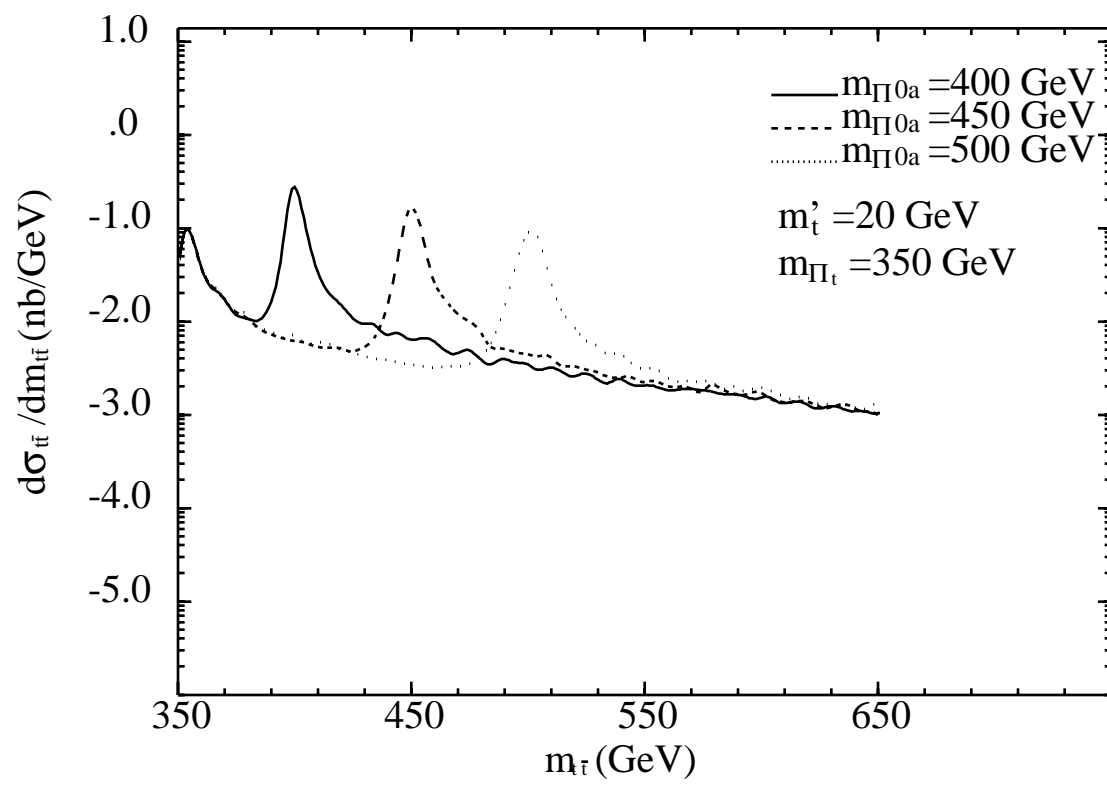


Fig. 9